



LCC - Q300-390

DOI: 10.6084/m9.figshare.5230339

## ANALYSIS OF SUBTLE CHANGES IN BIOMEDICAL SIGNALS

### BASED ON ENTROPY PHASE PORTRAIT

Fainzilberg Leonid<sup>1,2</sup>, Orikhovska Kseniia<sup>1</sup>, Vakhovskyi Ivan<sup>2</sup>

<sup>1</sup>International Research and Training Center for Information Technologies and Systems of National Academy of Sciences of Ukraine and Ministry of Education and Science of Ukraine (Kiev, Ukraine)

<sup>2</sup>National Technical University of Ukraine “Kiev Polytechnical Institute” (Kiev, Ukraine)

**Address for Correspondence:** Fainzilberg Leonid, chief Researcher, Str. Heroyiv Dnipra, 36-17, Kyiv, Ukraine, 04214

Institutional affiliation: prosp. Glushkova, 40, Kyiv, 03680

Email: kseniaor@gmail.com

**Abstract.** A new method for evaluating subtle changes in biomedical signals, caused by external influences on the human organism, is proposed. The method is based on the analysis of chaoticness of the studied parameter, which is calculated in a sliding window along an array of observed values using different entropy estimations. A distinctive feature of the method is the transition from the calculated entropies to their mapping on the phase plane and estimation of the integral parameters of the obtained graphic image (the entropy phase portrait), in particular, the area of the convex hull.

The diagnostic value of the proposed approach in the processing of real clinical data was demonstrated, obtained under conditions of increasing physical activity, coronary artery bypass surgery and intravenous drip infusion.

**Keywords:** ECG; Heart rate; Phase portrait; Entropy.

**Introduction.** Modern systems of medical diagnostics are often based on computer processing of physiological signals that are generated by the human organism in the course of its functioning. For example, an electrocardiogram (ECG), which carries information about changes in the electrical activity of the heart, has been one of the most accessible and widespread methods of functional diagnostics in cardiology for more than a hundred years.

The rapid development of computer and information technology has laid the foundation for a new industry – computer electrocardiography. Certainly, digital electrocardiographs that support decision-

making by a cardiologist facilitate the work of medical staff and shorten the time of obtaining the diagnosis results.

At the same time, as experts note, computer implementation of *traditional approaches* to ECG processing in the time domain does not lead to the achievement of a more important goal – increasing the reliability of diagnostic results. In addition, experienced clinicians still prefer a visual interpretation of the ECG, not fully trusting computer algorithms, which sometimes lead to errors at the stage of measuring diagnostic features [1].

Doctors are guided not only by the values of diagnostic signs, but also take into account the general clinical picture and take "informal" decisions, relying on their previous experience and intuition while making a diagnosis. Therefore, in medical practice, cases where several experienced cardiologists interpret the same ECG in different ways are well known.

Computer electrocardiography is based on formal algorithms for analyzing the deviations of ECG values from population norms. In this case, both gross and subtle deviations of the ECG form have diagnostic value.

Gross deviations are a pathological (wide and deep)  $Q$ -wave, a significantly expanded  $QRS$ -complex and a number of other ECG diagnostic signs, the analysis of which is not very difficult either in visual or in computer analysis of ECG. Significantly greater problems are caused by computer analysis of subtle signal changes such as alternation or symmetrization of the  $T$ -wave, which are almost invisible in the visual analysis of the ECG, but carry important diagnostic information.

Scientists are constantly looking for *new* approaches to the analysis of subtle changes in the ECG-signal. One such innovative approach is phasegraphy, which is based on the transition from a scalar signal  $z(t)$  in any of the leads to its processing on the phase plane  $z(t), \dot{z}(t)$ , where  $\dot{z}(t)$  – is assessment of the rate of change of heart electrical activity [2].

It should be emphasized that such an approach *fundamentally* distinguishes a phasegraphy from analogous methods [3], based on the reflection signal in a plane with coordinates  $z(t), z(t - \tau)$ , where  $\tau$  – is time lag. This difference allowed expanding the system of ECG diagnostic features, based on the evaluation of the speed characteristics of the process, and thereby improving the sensitivity and specificity of ECG diagnostics.

The phasegraphy method is implemented in the domestic portable complex FAZAGRAPH<sup>®</sup>, which provided a reliable determination of the  $\beta_T$  parameter that describes the symmetry of the repolarization section of the averaged phase trajectory [4]. Clinical studies have confirmed that the  $\beta_T$  parameter, which until recently was underestimated by physicians in the analysis of ECG, carries important diagnostic information on the initial signs of ischemic changes in the myocardium [5,6].

The interpretive possibilities of the phasegraphy are constantly expanding. Recently, for studying the dynamics of complex biomedical systems behavior, the methods of synergetics and the theory of dynamic chaos have become popular [7]. Thanks to synergetics, it was possible to move on to understanding how in open chaotic systems ordered structures appear spontaneously as a result of nonlinear processes. For example, in [8] carried out the study of the researching some aspects of human bioelectrical activity from the deterministic chaos positions.

According to [9], not only the entropy itself but also the nature of its change in time has important information about the system properties. Based on the analysis of the entropy changing form, Anishchenko [10] found gender differences in the body's response to stressful environmental influences. In [11] a number of interesting results were obtained using the entropy method in a complex assessment of cardiovascular risk factors dynamics.

The composition of the phasegraphy includes an additional software module that provides an estimation of the chaotic ECG parameters [12]. Further development of the entropy approach for the analysis of the chaotic ECGs and other biomedical signals will provide additional information in assessing the subtle changes in the signal caused by external influences on the body (physical activity, drug therapy, surgical intervention, etc.), which means that it is an actual task both in scientific and applied importance.

**The purpose of the article** is to develop a new method for analyzing *subtle* ECG-signal changes based on sliding entropy in phase coordinates and practical testing of the method on clinical data.

**Materials and Methods.** Let the  $z(t)$  be ECG-signal, observed at discrete instants of time  $t_k \equiv k\Delta$ ,  $k = 1, \dots, K$  be represented by a finite sequence of individual cycles  $z_1(k)$ ,  $z_2(k)$ ,  $\dots$ ,  $z_M(k)$ , where  $\Delta$  – is the quantization step in time,  $M$  – is the total number of cycles.

Following [13], we approximate each  $m$ th  $z_m(k)$  cycle by some  $\varphi(k, \theta_1, \dots, \theta_G)$  function specified up to a finite number of unknown parameters  $\theta_1, \dots, \theta_G$ . To determine the optimal values of these parameters, we use the criterion of the minimum sum of deviations squares

$$Cr = \sum_{k=1}^{K_m} [\varphi(k, \theta_1, \dots, \theta_G) - z_m(k)]^2 \rightarrow \min, \quad (1)$$

where  $K_m$  is the number of discrete samples  $z(t)$  on the  $m$ th cycle.

In this case, each separate cycle  $z_m(k)$  represents a point (vector)  $\vec{\theta}_m = (\theta_{1m}, \dots, \theta_{Gm})$  in the  $G$ -dimensional parameter space, and the sequence of observable cycles  $z_1(k), z_2(k), \dots, z_m(k)$  generates in this space a phase trajectory that uniquely corresponds to the observed signal  $z(t)$ .

As a function that describes with reasonable accuracy the cycles of real ECGs, we will use the sum of asymmetric Gaussian functions

$$\varphi(k) = \sum_v A_v \exp\left[-\frac{(k - \mu_v)^2}{2[\sigma_v(k)]^2}\right], \quad v \in \{P, Q, R, S, ST, T\}, \quad (2)$$

in which the parameters  $A_v$  and  $\mu_v$  determine the values of the amplitudes and instants of time, when the  $v$ th fragment assumes extreme values, and the function  $b_v(k)$  is determined by the expression

$$b_v(t) = \begin{cases} b_v^{(1)} & \forall t \leq \mu_v, \\ b_v^{(2)} & \forall t > \mu_v. \end{cases} \quad (3)$$

Under the  $b_v^{(1)} \neq b_v^{(2)}$  function (3) makes it possible to describe asymmetrical fragments, in particular, an asymmetric  $T$ -wave, if  $b_T^{(1)} \neq b_T^{(2)}$ .

Thus, the  $v$ th informative fragment  $v \in \{P, Q, R, S, ST, T\}$  of the ECG cycle can be represented by only four parameters  $A_v, \mu_v, b_v^{(1)}, b_v^{(2)}$ , and each  $m$ th cycle can be represented by a point in the 24-dimensional parameter space, i.e. vector

$$\vec{\theta}_m = (A_p, b_p^{(1)}, b_p^{(2)}, \mu_p, \dots, A_T, b_T^{(1)}, b_T^{(2)}, \mu_T), \quad m = 1, \dots, M \quad (4)$$

Since the Gaussian function is mainly concentrated on the 3-sigma interval, it is legitimate to assume that the moments of the beginning  $t_v^{(1)}$  and the ending  $t_v^{(2)}$  of each  $v$ th fragment of the ECG are related to the parameters  $\sigma_v^{(1)}$ ,  $\sigma_v^{(2)}$  and  $\mu_v$  as follows:

$$t_v^{(1)} = \mu_v - 3\sigma_v^{(1)}, \tag{5}$$

$$t_v^{(2)} = \mu_v + 3\sigma_v^{(2)}. \tag{6}$$

It follows that the main ECG diagnostic parameters, including an additional  $\beta_T$  parameter of the repolarization section symmetry, can be calculated using the ratios given in Table 1.

Experimental studies have shown [14] that even with a high level of interference, the error in estimating these real ECG parameters of various shapes do not exceed 1 %.

Table 1

Calculation formulas of diagnostic parameters

Parameters	Calculation formulas
$Q$ -wave duration	$\Delta_Q \triangleq t_Q^{(2)} - t_Q^{(1)} = 3(\sigma_Q^{(1)} + \sigma_Q^{(2)})$
$PQ$ -interval duration	$\Delta_{PQ} \triangleq t_Q^{(1)} - t_P^{(1)} = \mu_Q - \mu_P + 3(\sigma_P^{(1)} - \sigma_Q^{(1)})$
$QT$ -interval duration	$\Delta_{QT} \triangleq t_T^{(2)} - t_Q^{(1)} = \mu_T - \mu_Q + 3(\sigma_Q^{(1)} + \sigma_T^{(2)})$
$QRS$ -complex duration	$\Delta_{QRS} \triangleq t_S^{(2)} - t_Q^{(1)} = \mu_S - \mu_Q + 3(\sigma_Q^{(1)} + \sigma_S^{(2)})$
$RR$ -interval duration	$\Delta_{RR} = \mu_R[m] - \mu_R[m-1], \quad m \geq 2$
$Q$ -wave depth	$A_Q$
$ST$ -segment displacement	$A_{ST}$
$T$ -wave amplitude	$A_T$
$T$ -wave symmetry	$\beta_T = \frac{\sigma_T^{(2)}}{\sigma_T^{(1)}}$

The theory of chaos and synergetics allows us to more fully reveal and analyze the mechanisms of living complex system functioning that combines features of order and disorder, certainty and uncertainty, organization and disorganization [7].

For an integrated assessment of the parameters chaotic dynamics during the ECG recording, the following method is proposed.

### MATHEMATICAL FOUNDATIONS OF THE PROPOSED METHOD

It is needed to estimate the chaoticness of the time series

$$a_1, a_2, \dots, a_M, \quad (13)$$

elements of which are sequences of any parameters values indicated in Table 1, for example, a sequence of  $RR$ -interval values or a sequence of parameter  $\beta_T$  values from cycle to cycle.

We divide the series (13) into  $L$  consecutive windows containing  $W$  points, in each  $l$ th window we estimate the chaoticness  $H_l$  of the explored parameter values and calculate the ratio of  $H_l$  to the elements chaoticness  $H_1$  in the first window:

$$h_l = \frac{H_l}{H_1} \cdot 100\%, \quad l=1, \dots, L, \quad (14)$$

assuming, that  $H_1 \neq 0$ .

Any mathematical method for analyzing the chaoticness of dynamic series elements can be used to estimate  $H_l$ . In particular, such estimation can be carried out on the basis of the Shannon entropy calculation

$$H_l = -\sum_{j=1}^J p_{jl} \log p_{jl}, \quad (15)$$

where  $p_{jl}$  – frequency of hitting the  $j$  th interval  $\Delta_j = [a_j^-, a_j^+]$ ,  $j = 1, \dots, J$  of the time series values observed in the  $l$  th window. The thresholds  $a_j^-, a_j^+$  of the intervals  $\Delta_j$ , including the alternating elements  $a_i$ , determine a ratio

$$a_j^- = \min a_i + \delta(j-1), \quad a_j^+ = \min a_i + \delta j, \quad j = 1, \dots, J, \quad (16)$$

where  $\delta$  – specified threshold of insensitivity to changes in the parameter.

The procedure (14) can be implemented by shifting the  $l + 1$  th window towards  $l$  th at the width of window  $W$  or when the windows are shifted by one point (sliding window mode). It is clear that in the second case the amount of computation required is greater, but the graph of entropy change will be smoother. In this case, the form of such graph depends on the width of the window  $W$  and the threshold  $\delta$  (Fig. 1).

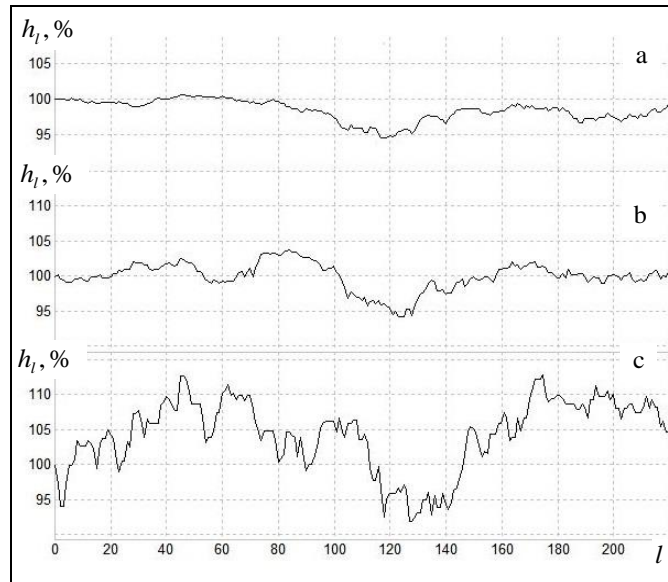


Fig.1. Sliding entropy graphs  $h(l)$  by estimation  $\beta_T$  chaoticness:

a:  $W = 100$  pts.,  $\delta = 0,1$  un.; b:  $W = 60$  pts.,  $\delta = 0,04$  un.; c:  $W = 30$  pts.,  $\delta = 0,02$  un.;

For the integral chaotic estimation of the parameter during ECG observation, it is proposed to move from a series of discrete values  $h(l)$  calculated by the sliding window method to a phase portrait of entropy on the  $h(l), \dot{h}(l)$  plane, where  $\dot{h}(l)$  is an estimation of the first derivative of  $h(l)$  at the  $l$  th point.

Despite the fact that the procedure of numerical differentiation of noisy data refers to an incorrectly posed mathematical problem, the application of special filtration and regularization procedures [15] made it possible to obtain acceptable estimates of the derivative  $\dot{h}(l)$ . As a result, it is possible to build an evident graphic representation of the phase portrait entropy as points on the  $h(l), \dot{h}(l)$  plane (Fig. 2).

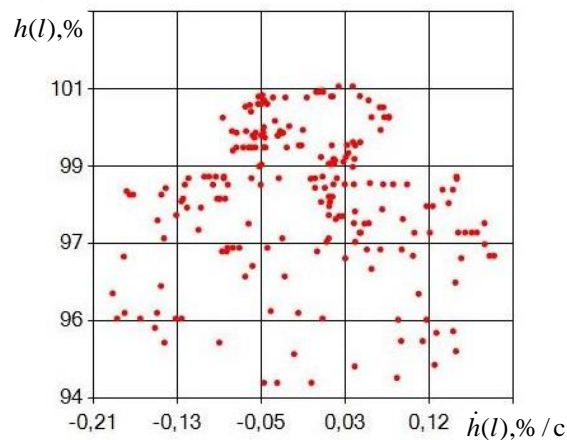


Fig.2. Phase portrait of the  $\beta_T$  sliding entropy (real ECG).

It should be noted that the classical Shannon entropy (15) is invariant under the permutations of the elements in the window. For example, two sequences - regular

$$1, 0, 1, 0, 1, 0, 1, 0, 1, 0, 1, 0$$

and chaotic

$$0, 1, 0, 0, 0, 0, 1, 1, 0, 1, 1, 1, 0, 1$$

will have the same entropy values  $H = 1$ .

Therefore, for a deeper study of chaotic dynamics, it is possible to calculate permutation entropy [18] in each  $l$  th window, instead of estimation (15), which is based on the analysis of the characteristic patterns shape.



In order to realize this possibility, we modernized the well-known procedure of calculating the permutation entropy, and evaluated five classes of patterns using the three successive values of  $a_{m-1}$ ,  $a_m$ ,  $a_{m+1}$  of the time series (13) (Fig. 3).

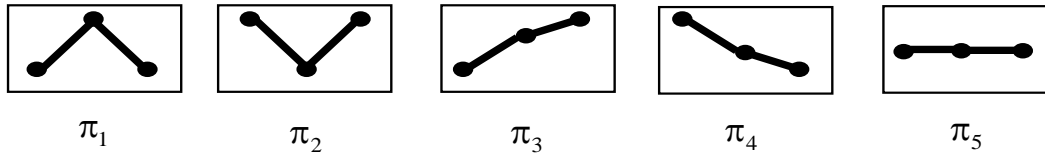


Fig.3. Five classes of modernized permutation entropy patterns.

The permutation entropy is calculated by the formula

$$PE_l = - \sum_{j=1}^5 p(\pi_{j_l}) \log_2 p(\pi_{j_l}), \quad (17)$$

in which  $p(\pi_j)$  is the frequency of the  $j$  th class pattern appearance in the  $l$  th window.

Classes of patterns are uniquely determined by sequential test of the following conditions:

class  $\pi_1$ , if  $(a_m - a_{m-1}) > h \wedge (a_m - a_{m+1}) > h$ ,

class  $\pi_2$ , if  $(a_{m-1} - a_m) > h \wedge (a_{m+1} - a_m) > h$ ,

class  $\pi_3$ , if  $(a_m - a_{m-1}) > h \vee (a_{m+1} - a_m) > h \vee (a_{m+1} - a_{m-1}) > h$ ,

class  $\pi_4$ , if  $(a_{m-1} - a_m) > h \vee (a_m - a_{m+1}) > h \vee (a_{m-1} - a_{m+1}) > h$ ,

class  $\pi_5$ , if none of the above relations holds,

in which  $h$  – is a given threshold of insensitivity to local changes in the signal.

The phase portrait can also be constructed on the basis of the approximate entropy [21] calculation and other known chaotic estimations, a review of which is presented in [12].

Note that the entropy change rate is actively studied in thermodynamic systems [16]. Despite the fact that the question of the relationship between the thermodynamic Boltzmann entropy and the Shannon

entropy for the information processes description is still the subject of scientific discussions, such analogies are still useful.

Relying on a number of fundamental ideas, contained in the papers of I.R. Prigogine [17], Y.L. Klimontovich [18], A.A. Khadartsev [19], A.A. Yashin [11], V.I. Shapovalov [9] and other scientists, it can be assumed that the shape of the entropy phase portrait and its "size" in the phase space carries additional information on the system-control capabilities of cardiohemodynamics.

For an integral estimation of the dynamics of parameter chaoticness, let's build in the normalized coordinates  $h(l), \dot{h}(l)$  the convex hull of the entropy phase portrait (Fig.5) and determine the area  $S$  of the resulting polygon, as well as the coordinates of the phase portrait gravity center  $X, Y$ .

Under certain conditions, there is an unambiguous connection between the Shannon entropy and the standard deviation (RMS). For example, with a normal distribution of the random variable, which generating the series (13), this connection can be described by the logarithmic dependence

$$H \cong 2,05 + \log_2 \text{RMS}. \quad (18)$$

Hence, it would seem that the results of the dynamic series variability analysis (13) will be equivalent if in the sliding windows, instead of entropy (15), calculate the RMS of the observed values.

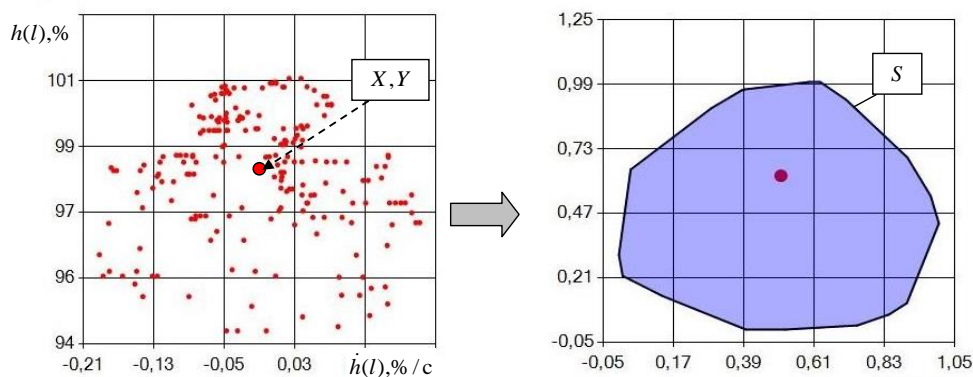


Fig.5. The phase portrait of the sliding entropy (left) and its convex hull (right).

At the same time, entropy, unlike RMS, does not depend on the values of the observed magnitude and therefore characterizes not so much the spread but the diversity of this quantity values [22]. Therefore, processing the real data will bring different results.

Fig. 6 shows graphs of Shannon entropy  $H$  and RMS change calculated by the same sequence of  $RR$ -interval.

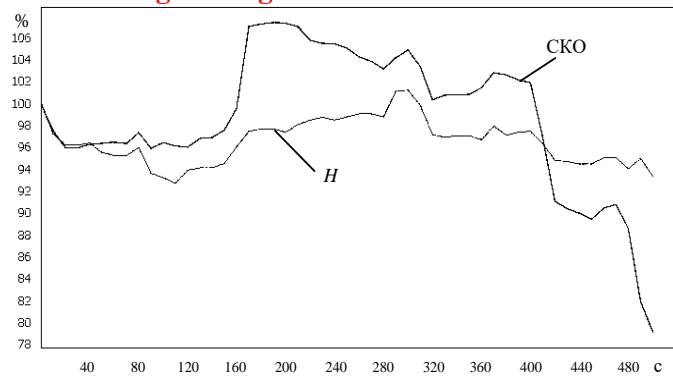


Fig.6. Graphs of entropy change  $H$  and standard deviation (RMS).

Let's consider the results demonstrating on the clinical data the possibility of the phasegraphy method for the subtle ECG changes analysis under various effects on the organism, including additional possibilities for analyzing the phase portrait of entropy (EPP).

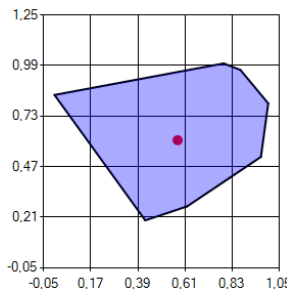
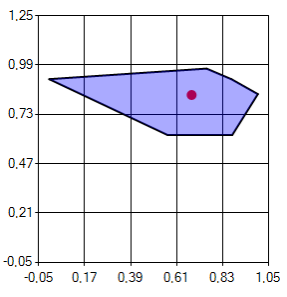
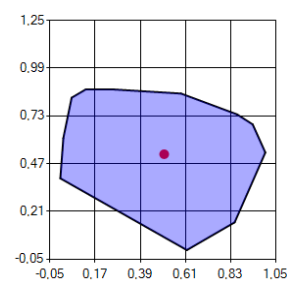
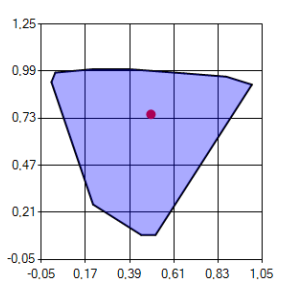
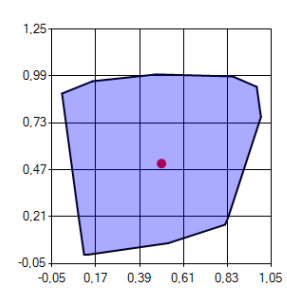
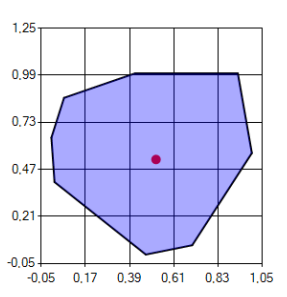
**Results.** Table 2 presents the results obtained during the testing a conditionally healthy volunteer for 44 years old on a treadmill. During testing, the speed of the belt reached 5.5 km/h, and the angle of inclination gradually increased to 14 %, which in the second stage ensured the metabolic equivalent MET = 10.2. After that, the test person rested for 3 minutes.

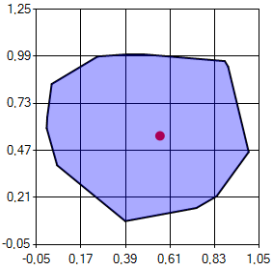
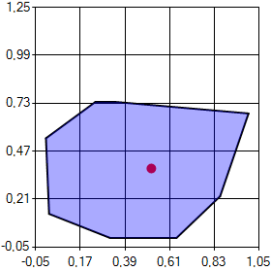
In the process of increasing the stress, the indicator  $SDNN$  (RMS of the  $RR$ -interval) decreased by 66 % (Fig. 7), which agrees with the known data on the increase in the sympathetic part of the autonomic nervous system under stress [23]. Simultaneously with the decrease in heart rate variability, the integral index  $S_{RR}$ , which, unlike  $SDNN$ , characterizes not the degree of dispersion, but the variety of  $RR$ -interval, increased by 60 %.

It can be assumed that the detected fact testifies that the healthy organism searches the most economical way for the heart rhythm regulation. Of course, such a hypothesis requires further studies.

Two other integral parameters characterizing the variability (RMS  $\beta_T$ ) and the variety ( $S_{\beta_T}$ ) of the  $T$ -wave symmetry values with increasing stress and rest were unidirectional (Fig. 8). At the same time, the changes in the integral index  $S_{\beta_T}$  at the first stage of the stress were more pronounced than the changes in the RMS  $\beta_T$ , but on the rest stage, the changes in the RMS  $\beta_T$  were more pronounced. The observed effect also requires additional study.

Dynamics of changes in integral parameters for a treadmill test

#	Stage	MET	CONVEX HULLS EPP		INTEGRAL PARAMETERS
			R-R interval	$\beta_T$ parameter	
1	2	3	4	5	6
0	Baseline	1			$S_{RR} = 0.497$ un. $X_{RR} = 0.576$ un. $Y_{RR} = 0.606$ un. $S_{\beta T} = 0.217$ un. $X_{\beta T} = 0.682$ un. $Y_{\beta T} = 0.831$ un. $SDNN = 58$ ms $CKO \beta_T = 0.02$ un.
1	Stress 3 min.	2.3			$S_{RR} = 0.617$ un. $X_{RR} = 0.507$ un. $Y_{RR} = 0.521$ un. $S_{\beta T} = 0.569$ un. $X_{\beta T} = 0.496$ un. $Y_{\beta T} = 0.751$ un. $SDNN = 32$ ms $CKO \beta_T = 0.04$ un.
2	Stress 15 min.	10.2			$S_{RR} = 0.794$ un. $X_{RR} = 0.5$ un. $Y_{RR} = 0.504$ un. $S_{\beta T} = 0.749$ un. $X_{\beta T} = 0.522$ un. $Y_{\beta T} = 0.524$ un. $SDNN = 20$ ms $CKO \beta_T = 0.09$ un.

1	2	3	4	5	6
3	Rest 3 min.	-			$S_{RR} = 0.716$ un. $X_{RR} = 0.561$ un. $Y_{RR} = 0.55$ un. $S_{\beta T} = 0.58$ un. $X_{\beta T} = 0.52$ un. $Y_{\beta T} = 0.376$ un. $SDNN = 92$ ms $CKO \beta_T = 0.08$ un.

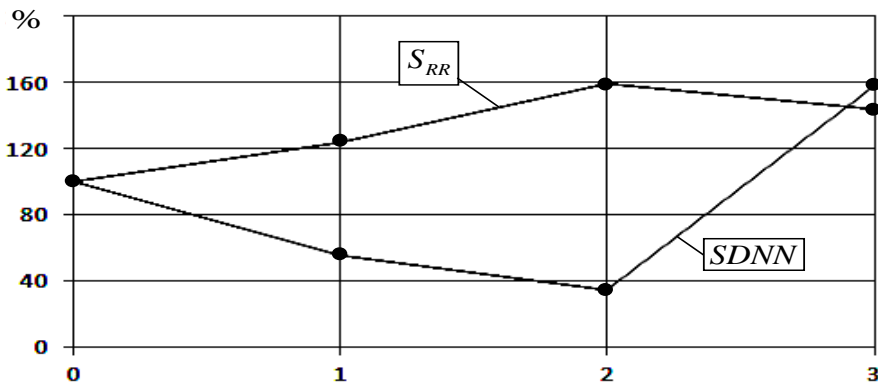


Fig.7. Dynamics of changes in the integral parameters of the heart rate

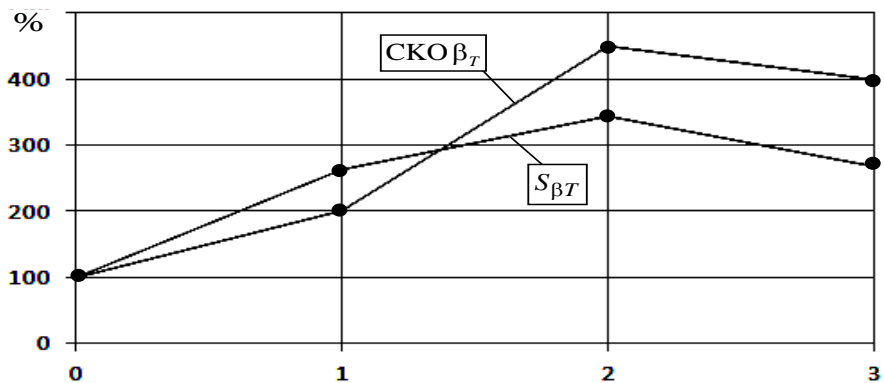


Fig.8. Dynamics of changes in the integral parameters of T-wave symmetry

Interesting results were obtained in the study of subtle ECG changes in patients with CAD whom coronary artery bypass surgery (CABG) was performed. Fig.9 shows the dynamics of the  $\beta_T$  parameter before and after the operative treatment of the patient M. 60 years old, owing to the lesion of the coronary arteries, three shunts were established.

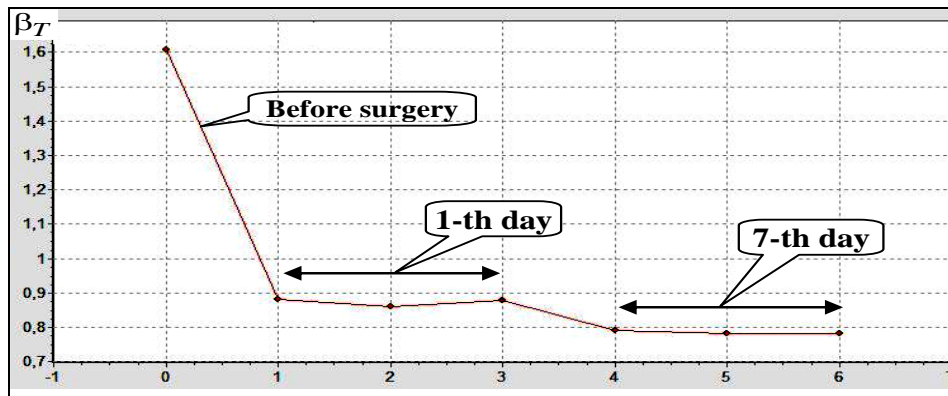


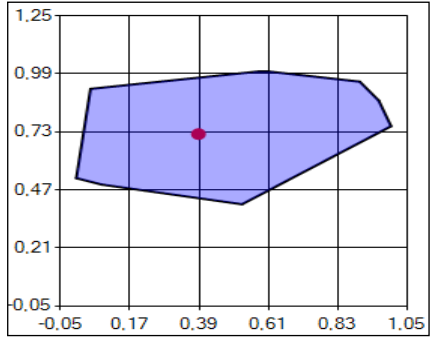
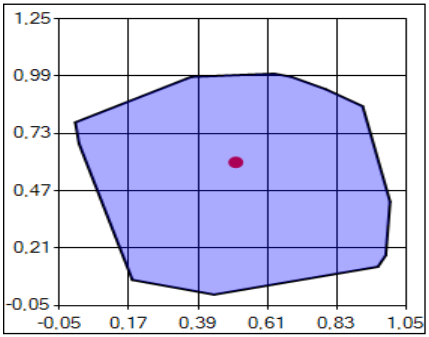
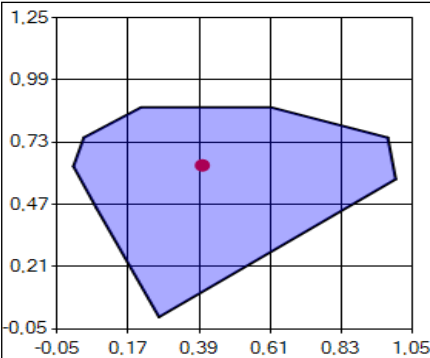
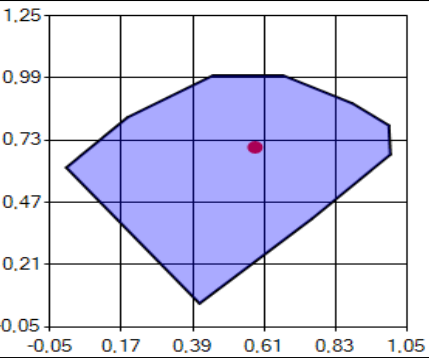
Fig.9. Dynamics of the  $\beta_T$  parameter before and after CABG surgery

The day before the surgery, the  $T$ -wave symmetry parameter was equal  $\beta_T = 1.6$  units, which was 60 % higher than the lower limit of pathological values ( $\beta_T = 1.05$  units). On the first day after the surgery, the  $\beta_T$  values were normalized ( $\beta_T \approx 0.9$  units), which indicates a blood flow restoration. On the 7th day after the surgery, the value of the parameter even more closely approached the norm and reached  $\beta_T = 0.8$  units, which is 50 % lower than the pathological value before the surgery. The patient successfully underwent the rehabilitation period and was discharged one week after the surgery.

It is noteworthy that against the background of the normalization of the  $\beta_T$  parameter, the dynamics of the entropy phase portraits were observed, which were constructed for the  $RR$ -interval and  $\beta_T$  parameter (Table 3). Already on the first day after the surgery, the EPP area  $S_{RR}$  of the convex hull of the  $RR$ -interval increased by almost 82 %, and the EPP area  $S_{\beta_T}$  of the convex hull  $\beta_T$  parameter increased by 2.4 %.

The detected properties indicate the possibility of using the phasegraphy method for evaluating subtle ECG changes before and after surgery and predicting the outcome of treatment.

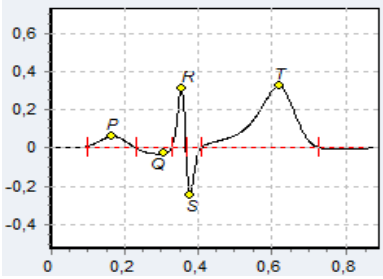
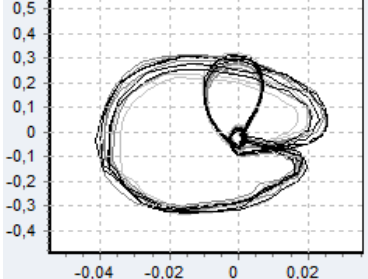
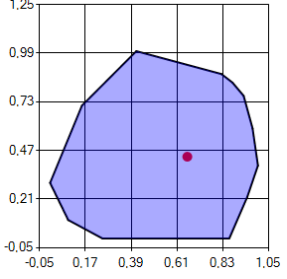
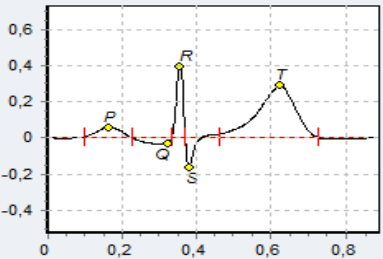
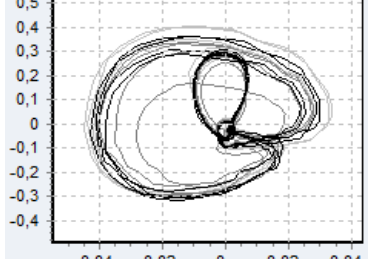
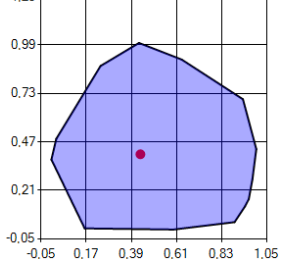
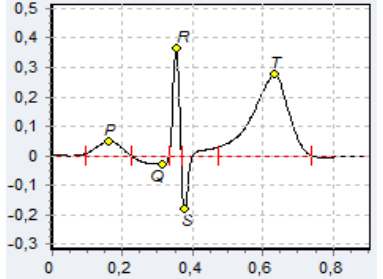
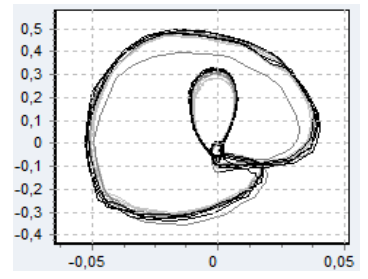
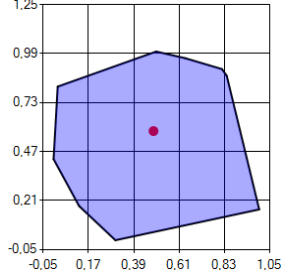
Dynamics of EPP before and after coronary artery bypass surgery (CABG)

	BEFORE SURGERY	1 DAY AFTER SURGERY
<b>RR - interval EPP</b>	 <p><math>S_{RR} = 0.431</math> units</p>	 <p><math>S_{RR} = 0.784</math> units</p>
<b><math>\beta_T</math> parameter EPP</b>	 <p><math>S_{\beta_T} = 0.535</math> units</p>	 <p><math>S_{\beta_T} = 0.548</math> units</p>

Many medications, including those used in cardiac practice, quite often (from 30 to 70 %) have side effects [24]. Therefore, the actual task is to assess the possibilities of phasegraphy in the analysis of subtle ECG changes directly in the process of intravenous therapy.

Table 4 shows the dynamics of changes in the parameters that were observed on the patient I. ECG (76 years old) in the process of intravenous therapy of Panangin and Mexicor medications.

Dynamics of ECG parameters during the first dropper

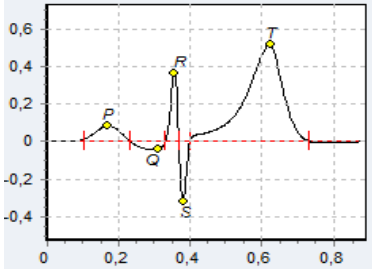
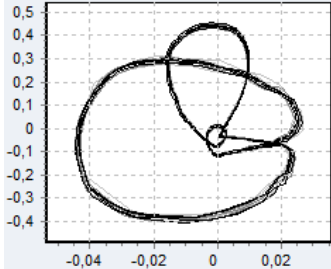
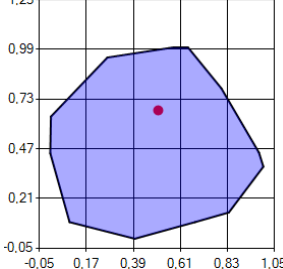
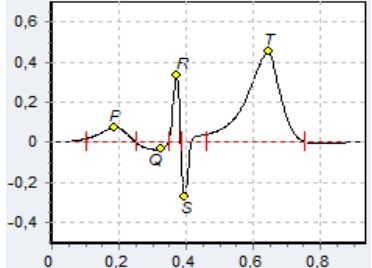
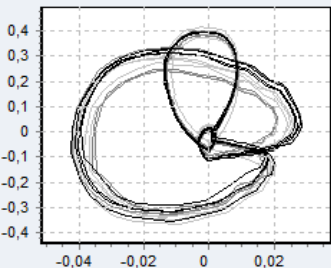
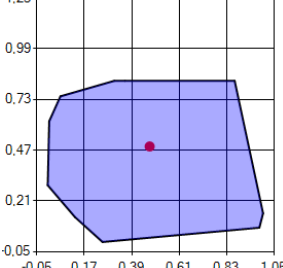
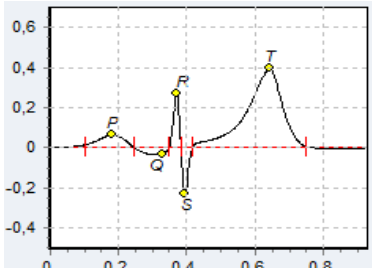
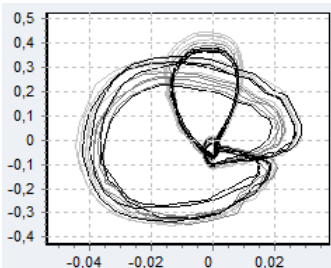
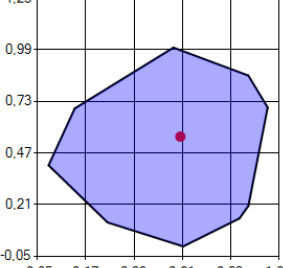
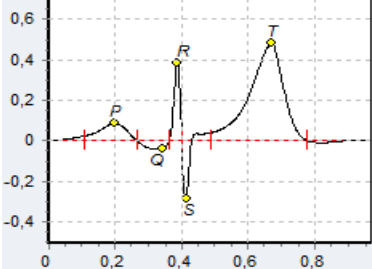
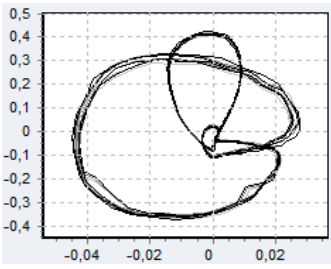
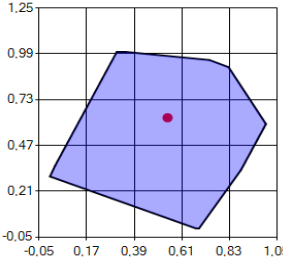
Time	AVERAGE CYCLE	ECG PHASE PORTRAIT	EPP convex hull of the $\beta_T$ parameter
15 min.	 <p><math>\beta_T = 0.65</math> units</p>	 <p><math>A_T = 0.44</math> mV.</p>	 <p><math>S_{\beta_T} = 0.764</math> units</p>
25 min.	 <p><math>\beta_T = 0.71</math> units</p>	 <p><math>A_T = 0.29</math> mV.</p>	 <p><math>S_{\beta_T} = 0.754</math> units</p>
40 min.	 <p><math>\beta_T = 0.64</math> units</p>	 <p><math>A_T = 0.28</math> mV.</p>	 <p><math>S_{\beta_T} = 0.744</math> units</p>

During the entire period of drug administration, the  $T$ -wave symmetry parameter was within the normal range:  $\beta_T = 0.653 \pm 0.014$  units. The EPP area of the  $\beta_T$  parameter was stable:  $S_{\beta_T} = 0.743 \pm 0.016$  units.

Two days later the patient was repeatedly treated with the same drugs (Table 5).



Dynamics of ECG parameters during the second dropper

Time	AVERAGE CYCLE	ECG PHASE PORTRAIT	EPP convex hull of the $\beta_T$ parameter
5 min.	 <p><math>\beta_T = 0.61</math> units</p>	 <p><math>A_T = 0.52</math> mV.</p>	 <p><math>S_{\beta_T} = 0.73</math> units</p>
10 min.	 <p><math>\beta_T = 0.65</math> units</p>	 <p><math>A_T = 0.44</math> mV.</p>	 <p><math>S_{\beta_T} = 0.697</math> units</p>
20 min.	 <p><math>\beta_T = 0.66</math> units</p>	 <p><math>A_T = 0.38</math> mV.</p>	 <p><math>S_{\beta_T} = 0.677</math> units</p>
30 min.	 <p><math>\beta_T = 0.63</math> units</p>	 <p><math>A_T = 0.47</math> mV.</p>	 <p><math>S_{\beta_T} = 0.65</math> units</p>

During the second dropper, the  $T$ -wave symmetry was also within the normal range:  $\beta_T = 0.604 \pm 0.006$  units. However, noticeable changes in the shape of the average cycle were observed. These changes are caused by a 36 % increase of the  $T$ -wave amplitude, which exceeded the  $R$ -wave amplitude and led to characteristic changes in the ECG phase portrait shape.

Interestingly, that the increase in  $T$ -wave amplitude, which is likely to be associated with hyperkalemia from excessive administration of potassium preparations, was accompanied by a monotonous decrease in the EPP area  $S_{\beta_T}$  of the  $\beta_T$  parameter by almost 11 %, i.e. decreasing  $T$ -wave form diversity from cycle to cycle.

A serious manifestation of cardiovascular diseases is sudden cardiac death, where a patient dies almost instantly (from a few seconds to an hour) after the onset of a heart attack. One of the sudden cardiac death predictors, which has recently gained wide popularity in clinical studies, is based on the detection of the electrical alternation of the heart, which on the ECG is manifested by the elements alternation, for example, in alternating  $RR$ -interval of different duration.

Computer analysis of the alternation becomes an important characteristic of modern medical diagnostic systems. Currently, according to experts, existing computer algorithms do not provide the required reliability of detection of this effect in real clinical conditions.

We will show that the proposed method makes it possible to detect subtle changes in the signal caused by the cardiac alternation effect and to distinguish such changes from externally similar microvibrations of ECG elements not related to this effect.

Fig.10 shows the ECGs of two patients who have changes in the duration of the  $RR$ -interval. One of the ECGs belongs to a conditionally healthy man of 32 years old, the second ECG belongs to a woman of 68 years old, and who has the heart electrical alternation.

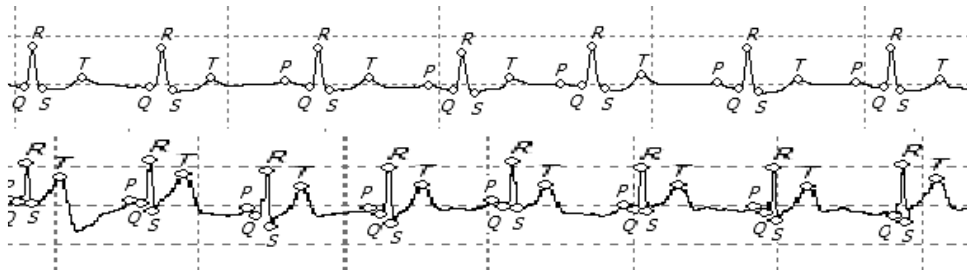


Fig.10. Real ECGs of a conditionally healthy patient (above) and a patient with an  $RR$ -interval alternation (below)

As you can see, the ECGs practically do not differ in the signal form. Despite this, differences in rhythm are clearly visible on the rhythmograms (Fig. 11), which are based on these ECGs. Note that the values of the traditional statistical parameter of heart rate variability calculated by these rhythmograms are quite close: in a healthy patient  $SDNN = 50$  ms, and in a patient with an alternation  $SDNN = 62$  ms.

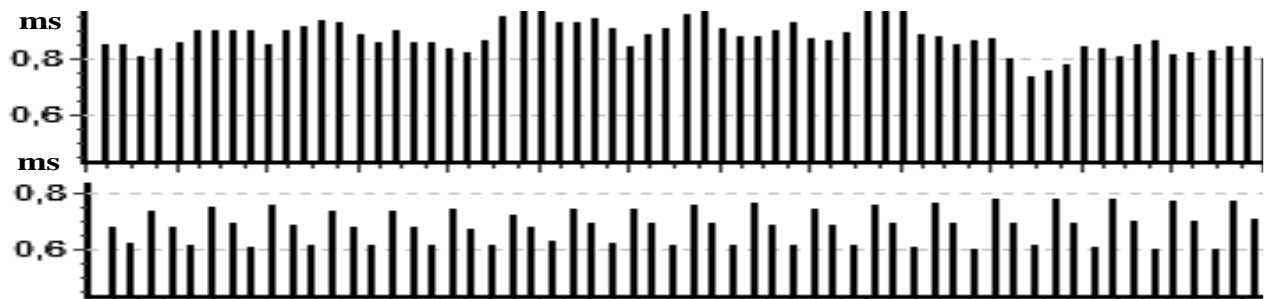
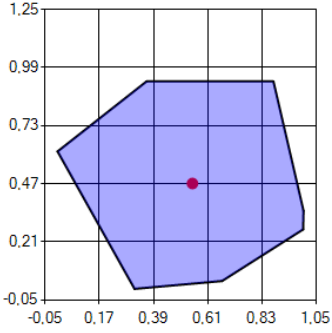
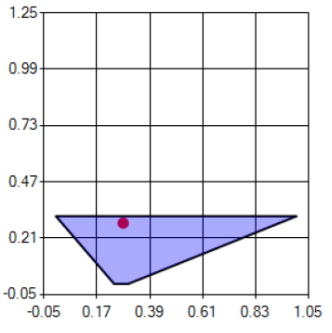


Fig.11. Real rhythmograms of a conditionally healthy patient (above) and a patient with an  $RR$ -interval alternation (below)

Analysis of the convex hulls area of the  $RR$ -interval entropy phase portrait was made to detect electrical alternation of the heart. In this case, in order to construct the EPP in (14) was used expression (17), instead of (15), providing an estimation of elements chaoticness in sliding windows on the basis of permutation entropy calculation. The results are shown in Table 6.

## Results of permutation entropy phase portraits analysis

Rhythmogram without $RR$ -interval alternation	Rhythmogram with $RR$ -interval alternation
	
$S_{RR} = 0.637$ units $X_{RR} = 0.363$ units; $Y_{RR} = 0.466$ units	$S_{RR} = 0.165$ units $X_{RR} = 0.279$ units; $Y_{RR} = 0.28$ units

As can be seen from Table 6, on the rhythmogram with electric alternation, the area of the convex phase portrait hull of the  $RR$ -interval permutation entropy was almost 4 times less than on the healthy patient rhythmogram, although both rhythmograms had similar  $RR$ -interval mean square deviations (traditional  $SDNN$  parameter).

Thus, the change in the integral  $S_{RR}$  parameter carries important diagnostic information about the reduction of the chaotic heart rhythm, which caused by the heart electrical alternation. Significantly changed the other two integral EPP parameters: a decrease of  $X_{RR}$  by 23.1 % and  $Y_{RR}$  by 39.9 %.

The analysis of integral parameters of the phase portrait of permutational entropy can give important information in the differential diagnosis of other cardiac rhythm disturbances, which will be the subject of our further research.

**Conclusion.** The article shows that the area of the phase portrait of entropy, calculated in sliding windows according to the heart rate and symmetry of the T-wave on consecutive cycles of the electrocardiogram, carries important information on the subtle changes in the ECG-signal caused by external effects on the body (treadmill test, drug and surgical treatment of cardiac patients) and can be used as an integral diagnostic parameter.

It is also shown that, based on the calculation of the area of the permutation entropy phase portrait, it is possible to reliably detect the effect of the electrical alternation of the heart on real signals that are

externally virtually indistinguishable from similar signals of a healthy person. This fact allows us to construct a threshold decision rule for assessing the risk of sudden cardiac death.

The received encouraging results after confirmation of their statistical reliability on representative samples of observations open new possibilities of medical diagnostics in cardiology.

**Conflict of interest statement:** The authors state that there are no conflicts of interest regarding the publication of this article.

**Author Contribution:** Conceptualization: Leonid Fainzilberg. Data curation: Kseniia Orikhovska. Formal analysis: Ivan Vakhovskyi. Writing – original draft: Leonid Fainzilberg. Writing – review & editing: Leonid Fainzilberg.

**ORCID**

**Fainzilberg Leonid** <http://orcid.org/0000-0002-3092-0794>

**REFERENCES:**

1. Oslopov VN, Sadykova AR, Fedoseeva TS. Limitations of automated computer electrocardiogram analysis. *Kazan med jour.* 2012;93(4):687-91.
2. Fainzilberg LS. *Fasegraphy basics.* Kyiv: Osvita Ukrainy; 2017. 264.
3. Frumin LL, Shtarck MB. About ECG phase portrait. *Avtometriya.* 1993;2:51-4.
4. Fainzilberg LS. *Computer diagnostics by phase portrait of electrocardiogram.* Kiev: Osvita Ukrainy; 2013. 191.
5. Fainzilberg LS. FAZAGRAF<sup>®</sup> is efficient information technology of ECG processing in the problem of ischemic cardiac disease screening. *Clinic Inform and Teled.* 2010;6(7):22-30.
6. Dyachuk DD, Kravchenko AM, Fainzilberg LS, Stanislavska SS, Korchinska ZA, Orikhovska KB, et al. Screening of myocardial ischemia myocardium by the assessment of repolarization phase. *Ukr cardio jour.* 2016 Jun;6:82-9.
7. Tuzov VV. Methods of synergetic. *Bibliosphere.* 2009;4:8–14.
8. Mayorov OY, Fenchenko VN. Improving the reliability of studies of deterministic chaos in the bioelectric activity (EEG, ECG and heart rate variability) methods of nonlinear analysis. *Clinic Inform and Teled.* 2009;6(6):10–7.
9. Shapovalov VI. About the fundamental laws of trend management. *Cont Scien.* 2005;2:2-11.
10. Anishchenko VS. Degree of randomness as a criterion for diagnosis [Internet]. Moscow (RU): Self-organization and non-equilibrium processes in physics, chemistry and biology; [updated 2006 Oct 31]; [about 4 screens]. Available from: [http://sinsam.kirsoft.com.ru/KSNews\\_331.htm](http://sinsam.kirsoft.com.ru/KSNews_331.htm).
11. Yashin AA. *Living matter. Physics of the alive and evolutionary processes.* Moscow: LKI; 2010. 264.
12. Fainzilberg LS, Orikhovska KB, Vakhovskyi IV. Assessment of chaotic fragments' shape of the single-channel electrocardiogram. *Cybernet and comp engineering.* 2016;183:4-24.
13. Fainzilberg LS. Generalized method of processing cyclic signals of complex form in multidimension space of patameters. *Jour of Automat and Inform Scien.* 2015 Jan;47(3):24-39.
14. Fainzilberg LS, Matushevych NA. An effective method for analysis of the diagnostic features based on noisy electrocardiogram. *Contr syst and machines.* 2016;2:76-84.
15. Fainzilberg LS. *Information technology for signal processing of complex shape. Theory and practice.* Kiev: Naukova Dumka; 2008. 333.
16. Tsirlin AM. *Optimal processes in irreversible thermodynamics and microeconomics.* Moscow: FIZMATLIT; 2003. 416.

17. Prigogine IR. The End of Certainty: Time, Chaos and the New Laws of Nature. Izhevsk: Science Publishing Center “Regular and Chaotic Dynamics”; 2000. 208.
18. Klimontovich YuL. Introduction to physics of open systems. Moscow: Janus-K; 2002. 284.
19. Khadartsev AA, Eskov VM. Internal diseases from the position of the theory of chaos and self-organization of systems (scientific review). Therapist. 2015;1:35-42.
20. Bandt C, Pompe B. Permutation entropy – a natural complexity measure for time series. Phys Rev Lett. 2002 Apr 29;88(17):174102.
21. Pincus SM. Approximate entropy as a measure of system complexity. Proc Natl Acad Sci USA. 1991 Mar 15;88(6):2297-301.
22. Gorban II. Entropy of uncertainty. Math Machines and Syst. 2013;2:105-17.
23. Dewey FE, Freeman JV, Engel G, Oviedo R, Abrol N, Ahmed N, et al. Novel predictor of prognosis from exercise stress testing: heart rate variability response to the exercise treadmill test. Amer Heart Jour. 2007;153(2):281-8.
24. Vlasova IV. There are more and more side effects in drugs. Commerc Biotech. 2007;10:14-9.